Microelectronic Engineering 216 (2019) 111047

Contents lists available at ScienceDirect

Microelectronic Engineering

journal homepage: www.elsevier.com/locate/mee

Research paper

Silicon solar cell efficiency improvement employing photoluminescent properties of chlorophyll-A

Rosendo Lopez-Delgado[a,b,*], Miriam Tostado-Plascencia[c], Mario E. Álvarez-Ramos[b], Arturo Ayón[a]

[a] MEMS Research Lab, Department of Physics and Astronomy, University of Texas at San Antonio, San Antonio, TX 78249, USA
[b] Departamento de Física, Universidad de Sonora, Hermosillo, Son 83000, Mexico
[c] Departamento de Ciencias Naturales y Exactas, Centro Universitario Valles, Universidad de Guadalajara, Ameca, Jal 46600, Mexico

ARTICLE INFO

Keywords:
Solar cells
Photoluminescence
Chlorophyll

ABSTRACT

Photoluminescent materials have attracted attention as candidates to improve photovoltaic efficiencies as photon energy conversion films. However, most cases involve materials or methods with either high costs, toxicity or long processing times. In contrast, chlorophyll has drawn big interest due to its photoluminescent properties, in addition to the availability of the inexpensive natural sources. Here, we describe an affordable extraction method of chlorophyll-A from spinach leaves and its influence on the performance of silicon solar cells. The extracted compounds absorb photons in two regions centered at around 428 nm and 660 nm respectively, and subsequently reemit photons with a maximum intensity at 665 nm. The incorporation of this material as a photon manipulation layer on solar cells triggered improvements in their performance. Specifically, the experimental results showed increments in the power conversion efficiency (PCE) from 15.27% to 15.61% which represents an improvement of the order of 2.23% of the PCE of the solar cells employed. Even though the influence of chlorophyll on the photovoltaic performance was relatively small, the improvement was achieved employing a natural source and the observed results exhibit a very attractive potential of this strategy. Which could be conducive to the promotion of natural based photoluminescent materials due to its affordability and low impact to the environment.

1. Introduction

The global energy consumption is increasing due to population and economy growth, and, in fact, the worldwide consumption is projected to reach 27 TW by 2050 [1]. In order to satisfy the global energy demand while avoiding the deleterious effects associated with carbon emissions due to the extensive usage of fossil fuels, the utilization of renewable energy sources is expected to increase in the foreseeable future, particularly solar energy because it represents one of the most attractive alternatives to meet the aforementioned energy demand [1,2]. Current research efforts to improve the power conversion efficiency of photovoltaic devices have focused on a variety of methods including surface nanotexturization, antireflection coatings and surface passivation schemes, among others. However, the relatively limited absorption range of the materials employed in solar cell manufacturing introduces a fundamental efficiency limit [3–6]. In principle, only photons with energy greater than the bandgap can be absorbed by the material leading to the loss of relatively low energy photons, and on the other hand, photons with energies larger than the bandgap lose their excess energy in a process referred to as thermalization, producing a lower photovoltaic response compared to photons with a near-bandgap energy [5]. These fundamental losses can be ameliorated by the utilization of photoluminescent materials, for instance quantum dots, with either up or down energy conversion characteristics [7–11]. Semiconductor quantum dots have attracted attention as promising alternatives in photovoltaic devices in two main schemes, namely, as active layers involving electron or hole transport processes [12,13] and as photon downshifting layers [14–17]. However, in most cases, the materials and/or methods employed could present a challenge during manufacturing because of the production costs and/or processing times involved. Presently, silicon based solar cells predominate in the photovoltaic market mostly due to the prevalent fabrication and technology infrastructure. The research involving alternative technologies, focuses on improving the power conversion efficiency (PCE) by making heterojunction tandem solar cells [18], enhancing the absorption efficiency of thin-film solar cells through various photonic patterns [19,20], by multiple-exciton generation [21] or space separating quantum cutting [22], etc. In this background scenario, chlorophyll has

* Corresponding author at: MEMS Research Lab, Department of Physics and Astronomy, University of Texas at San Antonio, San Antonio, TX 78249, USA.
E-mail address: Rosendo.lopezdelgado@utsa.edu (R. Lopez-Delgado).

https://doi.org/10.1016/j.mee.2019.111047
Received 19 October 2018; Received in revised form 6 June 2019
Available online 15 June 2019

attracted interest in several fields of science not only because photosynthesis takes place in this molecule but also due to its unusual set of electrical, chemical, and medicinal properties. Whether as a standalone material, or as part of composite arrangements, applications have been found in various fields [23,24]. The study of the processes occurring during photosynthesis has led to the development of nanoscale synthetic structures for the absorption of light and the subsequent manipulation of the captured energy. Some reports indicate that the ideal structure for the light absorption resides in the porphyrins which exhibit the features of intense electronic absorption band, a relatively long fluorescence decay time, and unique electronic, magnetic and photophysical properties among others [25]. In fact, the process of capturing energy from light takes place mainly in chlorophyll-A [26,27] because this molecule contains the porphyrin ring [28]. Furthermore, chlorophyll-A can be extracted and even separated in its different pigments whose function is to expand the absorption spectrum of primary pigments. Once chlorophyll has been extracted from leaves, it can be used in combination with silicon solar cells to quantify prospective increases in the PCE. Therefore, we describe an affordable method to extract chlorophyll compounds that represents a promising and cost-effective alternative to obtain the photo luminescent materials required for PCE improvements in silicon-based solar cells. Chlorophyll has also been employed as an active material in the quest for new photovoltaic techniques, however, in spite of the attractiveness of such proposed methods, to date only relatively small PCE values have been reported [29,30]. In contrast, the idea discussed herein, involves the utilization of silicon solar cells as the base devices in conjunction with the photoluminescent properties of chlorophyll as a performance enhancer. The deployment of the organic down-shifting material discussed in this report, have effected increases of approximately 2.23% in the power conversion efficiency of the photovoltaic devices under consideration. Thus, the performance improvement observed could help in promoting the proliferation of solar cells.

2. Experimental

2.1. Chlorophyll extraction

Chlorophyll compounds were extracted from fresh spinach leaves by grinding, employing a porcelain mortar and pestle set. To this end, 2 g of spinach leaves were cut into approximately 0.5 cm^2 pieces and deposited in the mortar; 5 ml of a solvent was added (five different solvents were used independently), and the combination was grinded with the pestle producing a paste of solvent, chlorophyll and leaf fragments. Subsequently, 25 ml of solvent was added to dilute the plant paste. Petroleum ether, acetone, isopropyl alcohol, methanol and ethanol were used as solvents. Once the chlorophyll extract had been diluted, 24 ml were collected and centrifuged for 5 min at 10000 rpm to separate the remaining fragments of the spinach leaves. Then 18 ml were collected ensuring that no solid residues were present in the sample. UV–Vis absorption and emission spectroscopy were performed to the centrifuged samples to determine the influence of the different solvents on the optical properties of the chlorophyll compounds (Chlorophyll-A and Chlorophyll-B), namely, the wavelength position of the absorption peaks and photoluminescence maximum (see Fig. 1).

2.2. Chlorophyll A and B separation

Upon performing the optical characterization of the chlorophyll compounds, the solution in acetone was further processed to obtain two dissimilar solutions, one containing mostly chlorophyll-A and the other containing mostly Chlorophyll-B. The separation was achieved by taking advantage of the fact that both types of chlorophyll exhibit polarity and solubility differences. Specifically, the first step consisted on changing the solvent of the sample under consideration; this exchange was achieved by adding 30 ml of petroleum ether to the previously obtained solution and the new mixture was transferred to a chromatography column. Acetone is soluble in water, but chlorophyll is not, furthermore the water/acetone mix has a larger density and is not miscible with petroleum ether, thus, by slowly adding 35 ml of water over the walls of the column, the water mixed with the acetone and settled down at the bottom of the chromatography column creating a well-defined interface between the water/acetone solution and the chlorophyll-rich petroleum ether solution. The bottom part of the solution (i.e., water/acetone) was then extracted, and the process was repeated 3 times to remove all the remaining acetone in the solution. In order to separate the chlorophyll-A from chlorophyll-B, the second step involved the addition of 30 ml of methanol under stirring, since methanol has a greater density and is immiscible with petroleum ether, after allowing the solution to settle, the two chlorophyll solutions separate. Due to the difference in the polarity and solubility between Chlorophyll A and B, the top portion of the chlorophyll-rich petroleum ether solution will contain mostly chlorophyll-A (Chl-A), while the bottom part of methanol will be mostly chlorophyll-B (Chl-B).

2.3. UV–Vis characterization

The UV–Vis absorption spectra and the photoluminescent effects of the chlorophyll compounds were recorded using an Ocean Optics Flame-S-UV-VIS spectrometer. For the photoluminescent characterization, a monochromator employing an excitation wavelength of 400 nm was employed.

2.4. Ellipsometry

Ellipsometry measurements were carried out employing a variable angle spectroscopic ellipsometer WVASE, J.A. Woollam Co. The measurements were performed on pure PMMA and chlorophyll/PMMA films deposited on a silicon wafer, at an angle of incidence of 70° in the wavelength range of 300 nm to 1000 nm in steps of 10 nm. To obtain the chlorophyll/PMMA film, 1 ml of chlorophyll was prepared (20 μM), then the solvent was evaporated, and the chlorophyll was re-dispersed in 1 ml of PMMA (495 PMMA 2% in Anisole) to preserve the concentration. The Chl-A/PMMA mixture was deposited in the silicon wafer by spin coating technique at 1000 rpm for 60 s, finally the film was cured at 130 °C for 60 in a hotplate. The same deposition conditions were employed for the pure PMMA film. Before the PMMA or the chlorophyll/PMMA films were deposited, a spectroscopic scan was performed to obtain the thickness of the native oxide layer present in the silicon wafer which was employed after the deposit to create an appropriate ellipsometric model. To estimate the optical properties and thickness, a Si/SiO_2/(Chl-A/PMMA) model was analyzed with the WVASE software package.

2.5. Solar cell characterization

The Current–Voltage characteristics (I-V curves) of the silicon based solar cells were obtained characterized using an Oriel Sol2A solar simulator under AM1.5G illumination at standard testing conditions, i.e., 100 $mWcm^{-2}$ at room temperature. The external quantum efficiency (EQE) characterization was performed with a Newport External Quantum Efficiency Measurement System (QEPVSI-B) in the wavelength range of 300 to 1100 nm.

3. Results and discussion

3.1. Absorbance and photoluminescence

As shown in the Fig. 1, the influence of the different solvents employed in the extraction of the chlorophylls compound is reflected as a relatively small -but not negligible- shift in the position of the absorption and emission peaks. Thus, the position of the violet absorption

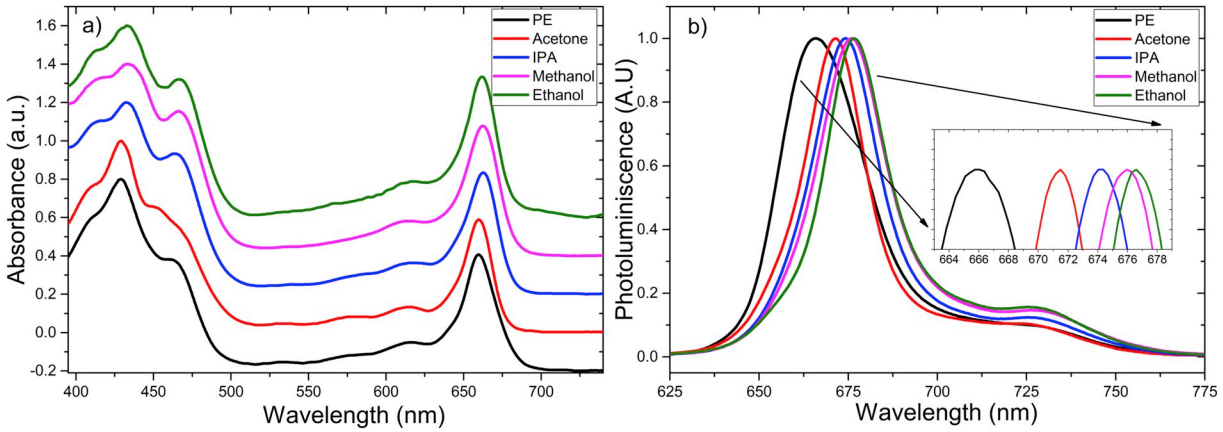

Fig. 1. (a) Absorbance and (b) Photoluminescence spectra of the extracted chlorophyll compound in different solvents, namely, petroleum ether (PE), acetone, isopropyl alcohol (IPA), methanol and ethanol.

peak shifts from 428 nm for petroleum ether to 434 nm for ethanol, while the position of the absorption red peak shifts from 660 nm for petroleum ether to 663 for methanol (see Fig. 1(a)). As shown in Fig. 1(b), a similar trend was observed for the photoluminescent maximum position which shifted from 665 nm for petroleum ether to 677 nm when ethanol was used.

Once the chlorophyll solutions were segregated, the absorbance and photoluminescence spectra were measured for each type of compound. Fig. 2 shows the absorbance of the original as well as the segregated solutions. Ostensibly, the purification/separation method resulted in a relatively pure sample of chlorophyll-A that displayed its characteristic violet and red absorption peaks [31], whereas the chlorophyll-B sample still exhibited a contribution from the presence of chlorophyll-A in the mixture. According to [32] the purification process for chlorophyll-B resulted in a sample composed by approximately 40% of Chl-A and 60% of Chl-B.

As previously mentioned, silicon solar cells have a lower photovoltaic response in the ultraviolet region of the electromagnetic spectrum compared to visible wavelengths. On the other hand (see Fig. 3) Chl-A has a maximum photon absorption near the UV (~428 nm), a minor absorption peak in the visible (660 nm) and a pronounced photoluminescent emission peak at ~665 nm. This property makes Chl-A a good candidate to have a beneficial influence as a photon manipulation layer to improve the performance of silicon based solar cells by means of converting high energy photons to lower energy photons, which

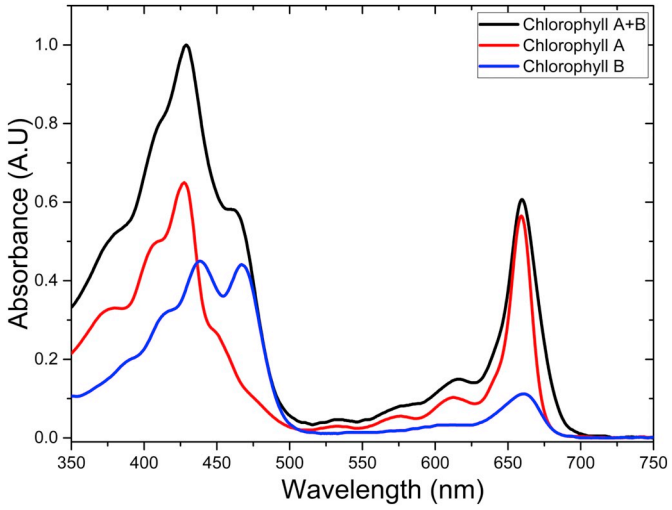

Fig. 2. Absorbance spectrum of the chlorophyll original mixture as well as the separated chlorophyll-A and chlorophyll-B solutions.

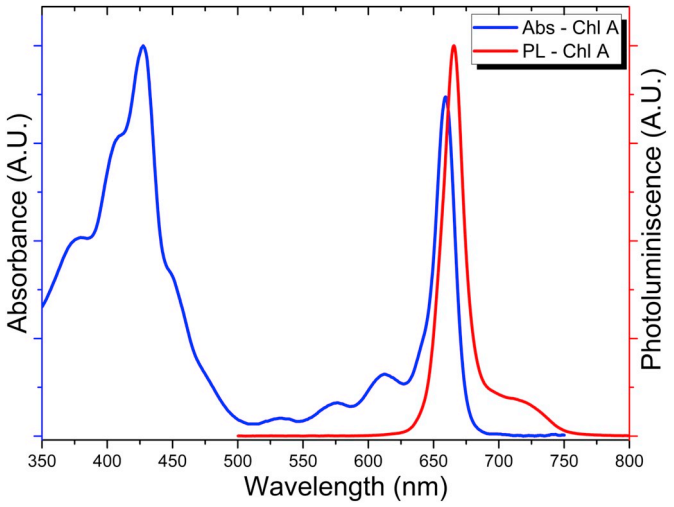

Fig. 3. Absorbance and photoluminescence spectrum of the obtained chlorophyll-A solution.

trigger a better response of the photovoltaic device. In order to study the influence chlorophyll has in the performance of solar cells, chlorophyll-A was further analyzed due to the higher purity obtained compared to chlorophyll-B, and also due to the observed optical properties.

In order to better understand the absorption and emission behavior of chlorophyll-A, a deconvolution of the signals was performed to estimate the energy levels involved in the absorbance and photoluminescence transitions. For the deconvolution of the absorbance spectrum, the measured data was divided in two sections corresponding to the violet and red absorption peaks, respectively (see Fig. 4). A similar deconvolution analysis was performed to the emission spectrum (see Fig. 5).

Employing the results obtained from the deconvolution of both the absorption and photoluminescence spectrum, a “Jablonski diagram” was employed to determine the energy transitions in the chlorophyll solutions (see Fig. 6).

Additionally, employing the data for the extinction coefficient of chlorophyll-A at both the violet and red absorption maxima [33,34], the concentration of the sample was calculated employing the Beer-Lambert law,

$$A = \epsilon c l \tag{1}$$

where A is the absorbance, ϵ is the molar extinction coefficient, c is the molar concentration and l is the optical path in the sample. Employing the concentration calculations, four different samples were prepared

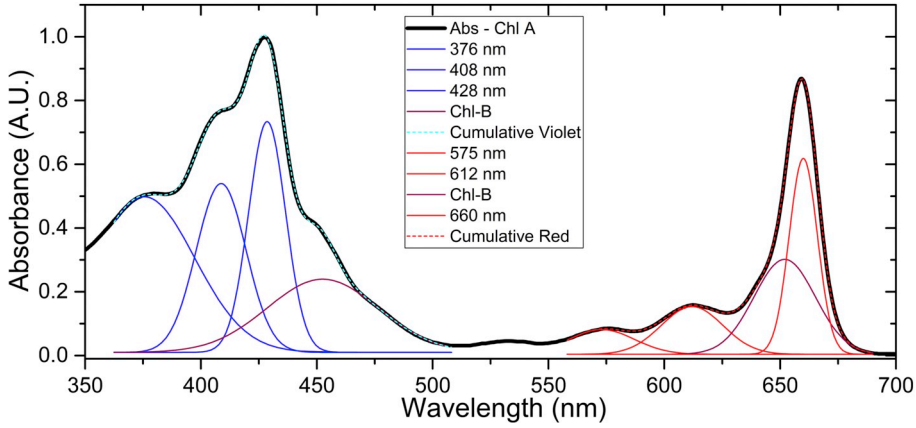

Fig. 4. Chlorophyll-A absorbance spectrum deconvolution and their maximum position wavelengths. It is also shown the remnant chlorophyll-B present in the solution.

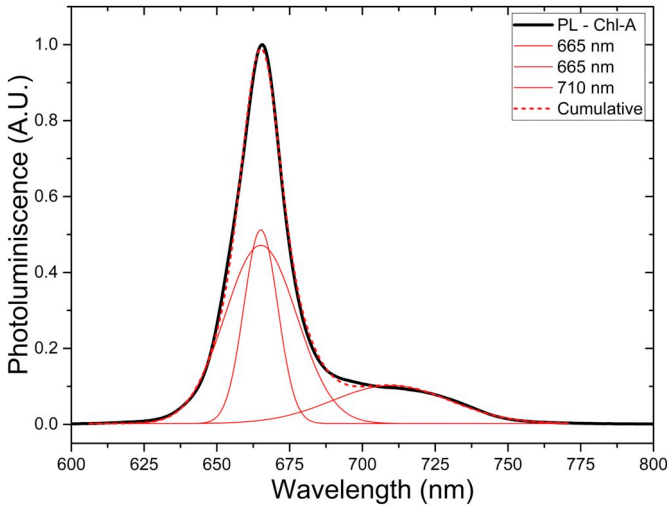

Fig. 5. Chlorophyll-A photoluminescence spectrum deconvolution and their maximum position wavelengths.

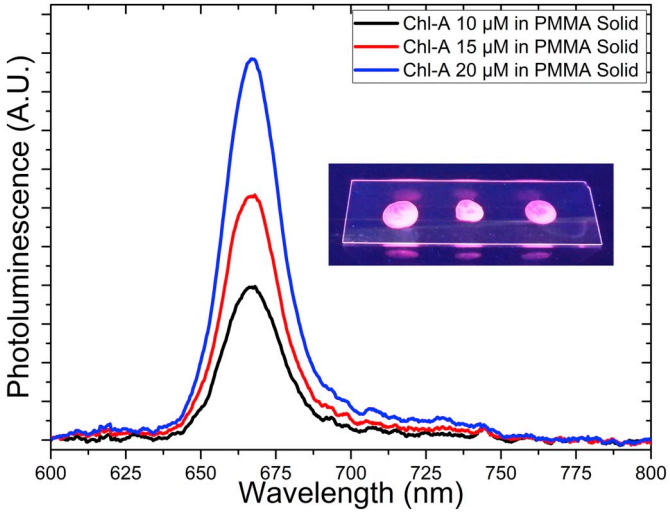

Fig. 7. Photoluminescent spectrum of Chl-A/PMMA after deposition and curing process. Inset is a picture of the dried droplets of the compound Chl-A/PMMA under UV light excitation. This result supports the idea of employing the chlorophyll/PMMA material as a photoluminescent layer on solar cells to improve the photons absorption, since the semitransparent solid film preserves the luminescent properties.

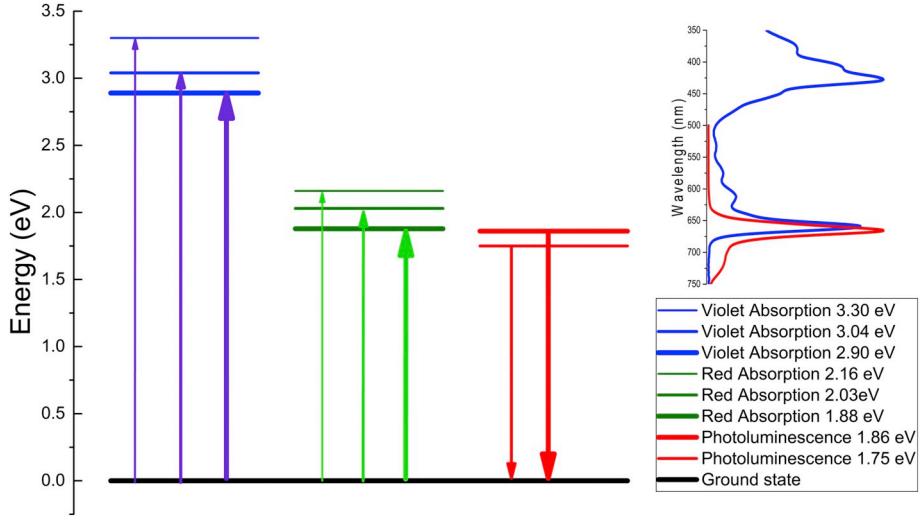

Fig. 6. "Jablonski diagram" of the energy levels in Chl-A and the transitions involved. The arrows pointing up represent absorption transitions while arrows pointing down represent emission transitions.

with concentrations of 5, 10, 15 and 20 μM. Subsequently, in order to deploy the photoluminescent material on functional solar cells, the transparent polymer polymethyl methacrylate (PMMA) was employed as a matrix host for chlorophyll-A. To this end, a chlorophyll-A/PMMA sample with a concentration of 20 μM chlorophyll was prepared by replacing the sample solvent for the same amount of PMMA (495 PMMA 2% in Anisole). As previously reported, the luminescent properties of chlorophyll depend on the solvent employed, hence, a further characterization was performed to corroborate that the photoluminescent effect was still preserved when the chlorophyll was dispersed in the PMMA matrix host. Fig. 7 displays the photoluminescent properties of chlorophyll-A dispersed in 495 PMMA 2% Anisole after the polymer was deposited and cured to remove all solvents.

3.2. Ellipsometry

The optical properties of the Chl-A/PMMA film were studied with ellipsometry in order to have a better estimation of the deposition thickness and optical characteristics. Ellipsometry is an optical technique employed to measure the variations in the amplitude and phase between the parallel R_p and perpendicular R_s components of a polarized beam of light after being reflected by a surface under study. The ratio between the intensities of the parallel and perpendicular components can be expressed in terms of the amplitude (Ψ) and phase (Δ) difference by the equation:

$$tan(\Psi)e^{i\Delta} = \frac{R_p}{R_s} \quad (2)$$

This effect represents an attractive characterization method since it provides useful information about the optical constants and thickness of the film studied. Thus, spectroscopic ellipsometry measurements were performed to study the effect of chlorophyll on the optical properties of the PMMA matrix host. A Si(600 μm)/SiO_2(1.5 nm) model was employed as a substrate. After the Si/SiO_2 substrate was characterized, a pure PMMA layer was deposited to serve as a reference, Fig. 8 shows the spectroscopic ellipsometry measurements for PMMA deposited on the Si/SiO_2 substrate. The measurements and model employed exhibit a reasonably good match, and a thickness of 97.1 ± 0.1 nm was obtained for the deposited pure PMMA layer. A Chlorophyll-A/PMMA film was studied with the same deposition parameters. Fig. 8 indicates that there is also a reasonably good agreement between the experimental data and the model, obtaining a thickness of 105.91 ± 0.09 nm.

Employing the aforementioned ellipsometry measurements, the refractive index of the PMMA and Chl-A/PMMA layers were also calculated. Fig. 9 displays the extracted values of the refractive index in the wavelength range of 300 nm to 1000 nm, as well as the results reported by Beadie in 2015 [35] for PMMA as a reference.

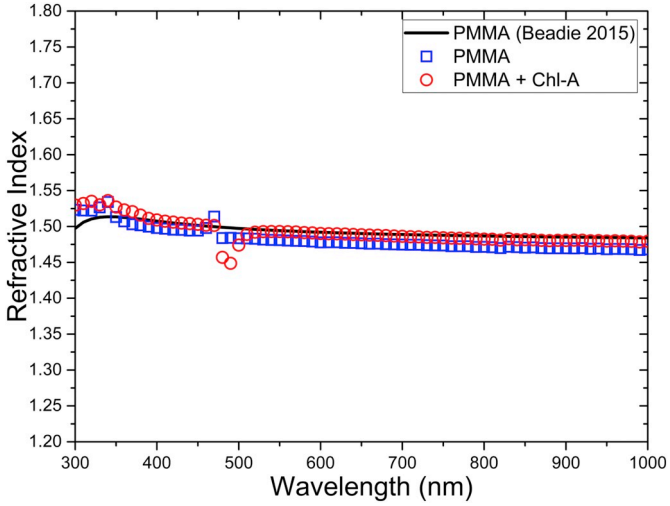

Fig. 9. Refractive index obtained from the spectroscopic ellipsometry measurements. Solid line represents the PMMA reference while the squares and circles represent the pure PMMA and Chl-A/PMMA films respectively.

The observations evince that even a 20 μM chlorophyll content in the PMMA host matrix, which was the highest Chl-A concentration employed in this study, has a relatively minor effect in the optical properties compared to a pure PMMA layer.

3.3. Effect of Chl-A/PMMA on solar cell performance

It is known that a typical silicon solar cell, has a decreasing photovoltaic response as the photon energy increases [5]. Therefore, chlorophyll-A and other luminescent materials exhibiting down-shifting effects, are good candidates to increase the performance of photovoltaic devices. In order to verify the anticipated positive influence of Chl-A in solar cells, semitransparent luminescent chlorophyll-A/PMMA films with concentrations of 5, 10, 15 and 20 μM were deployed on previously characterized devices. The study permitted the comparison of photovoltaic performance before and after the deposition of the Chl-A/PMMA films. Pure PMMA depositions were also carried out to ascertain whether the measured performance was due to the photoluminescent properties of chlorophyll. For each chlorophyll-A/PMMA concentration, four solar cells were characterized at three different times for a

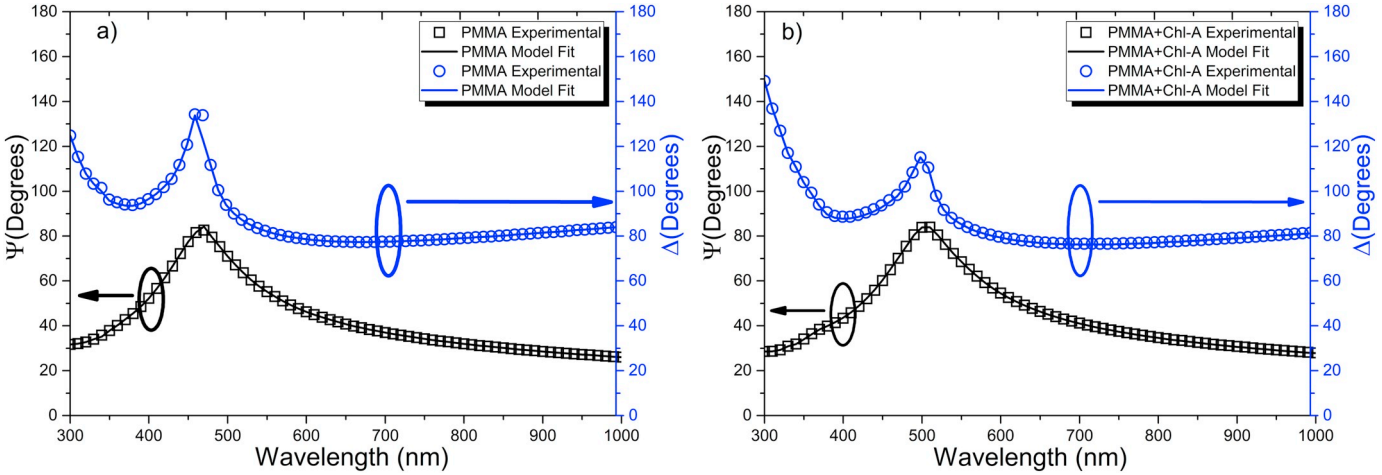

Fig. 8. Spectroscopic ellipsometry measurements of the deposited (a) PMMA and (b) Chl-A/PMMA films. In both figures, the squares and circles represent the experimental Ψ and Δ respectively while the continuous line represent the model fit.

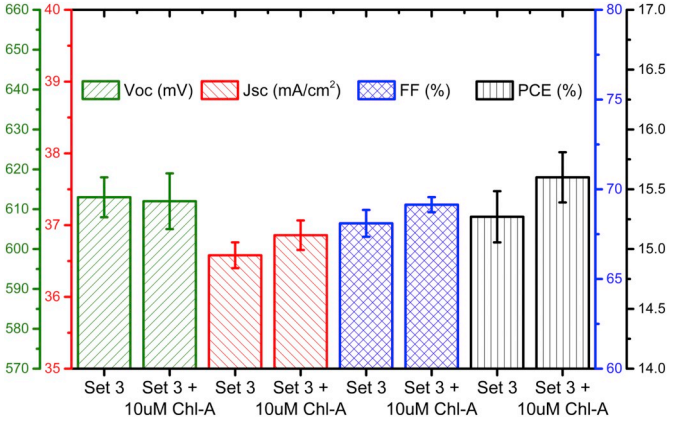

Fig. 10. Average of the photovoltaic parameters obtained from the J–V measurements before and after the deposition of the 10 μM Chl-A/PMMA film (vertical axis from left to right represent: voltage, current density, fill factor and PCE). The statistics present a confidence interval of 95% from the measured data.

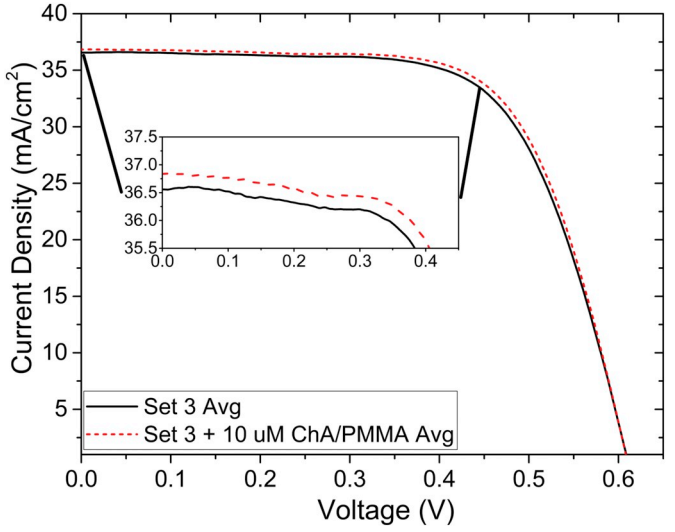

Fig. 11. Average of the current–voltage characteristics measured for the solar cell set before and after the deposition of the Chl-A/PMMA layer with a concentration of 10 μM (best concentration observed).

total of twelve independent measurements before and after the deposition of the different layers. Averages of the measured parameters are shown in Fig. 10.

The observations indicate that the deployment of a pure PMMA layer, ~100 nm thick, has a minor but not negligible negative effect on device performance. The average power conversion efficiency (PCE) of the set of solar cell measurements changed from 15.81% to 15.80% after the deposition of the PMMA layer. In comparison, the average PCE of the solar cells increased upon the deployment of most Chl-A/PMMA layers. Specifically, for the solar cell set with a 5 μM Chl-A concentration, a PCE increase from 15.62% to 15.76% was observed. The maximum improvement was found for a concentration of 10 μM, where the average PCE was increased from 15.27% to 15.61%. Fig. 11 displays the average I-V performance for the 10 μM Chl-A/PMMA concentration.

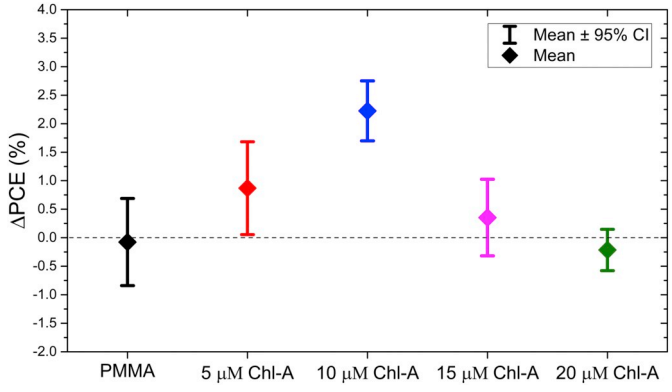

Fig. 12. Overall percental variation of the power conversion efficiency of the solar cell sets after the application of the respective films.

For the subsequent concentrations of 15 μM Chl-A/PMMA concentration, the photovoltaic improvement was noticeably smaller compared to the previous concentration of 10 μM. Specifically, the PCE varied from 15.49% to 15.55%, representing a total improvement of 0.39%, down from a 2.23% improvement with a 10 μM concentration. Finally, with a concentration of 20 μM, the measured PCE deteriorated even more. The collected PCE for this last Chl-A concentration changed from 15.34% to 15.31% after the deposition. The averages of the measured parameters are reported in Table 1.

As shown in Fig. 12, a photoluminescent layer, such as the Chl-A/PMMA film, have an important impact on the photovoltaic performance of silicon solar cells. It was found that the Chl-A concentration of the luminescent film has an evident relationship with the variation of the PCE measured, whereas a pure PMMA film has a minor effect. In fact, as the Chl-A concentration increases, the photovoltaic performance improves, reaching a maximum improvement of 2.23% with a 10 μM of Chl-A concentration. However, higher concentrations of Chl-A tend to decrease the improvement, up to a concentration of 20 μM where the performance was deteriorated. This effect is thought to be produced by an increase in the reflectivity and "shadowing" effects of the concentrated films. It is worth to mention that the present study was performed on fully functional silicon solar cells, and better improvements may be achieved by combining this technique with the proper antireflection coating methods or by pattering the photoluminescent structures.

Table 1
Influence of the different concentrations of Chl-A/PMMA layer on the photovoltaic performance of the silicon solar cells. The statistics present a confidence interval of 95% from the measured data.

	V_{oc} (mV)	J_{sc} (mA/cm^2)	FF (%)	PCE (%)	ΔPCE (%)
Solar Cell Set 1	621	37.20	68.46	15.81 ± 0.13	−0.06
Solar Cell Set 1 + PMMA	620	37.37	68.15	15.80 ± 0.17	
Solar Cell Set 2	621	37.27	67.53	15.62 ± 0.10	0.90
Solar Cell Set 2 + 5 μM Chl-A	622	37.40	67.74	15.76 ± 0.14	
Solar Cell Set 3	613	36.58	68.10	15.27 ± 0.21	2.23
Solar Cell Set 3 + 10 μM Chl-A	612	36.86	69.14	15.61 ± 0.21	
Solar Cell Set 4	614	36.83	68.56	15.49 ± 0.14	0.39
Solar Cell Set 4 + 15 μM Chl-A	614	37.07	68.36	15.55 ± 0.18	
Solar Cell Set 5	616	36.63	68.02	15.34 ± 0.18	−0.20
Solar Cell Set 5 + 20 μM Chl-A	614	36.97	67.46	15.31 ± 0.12	

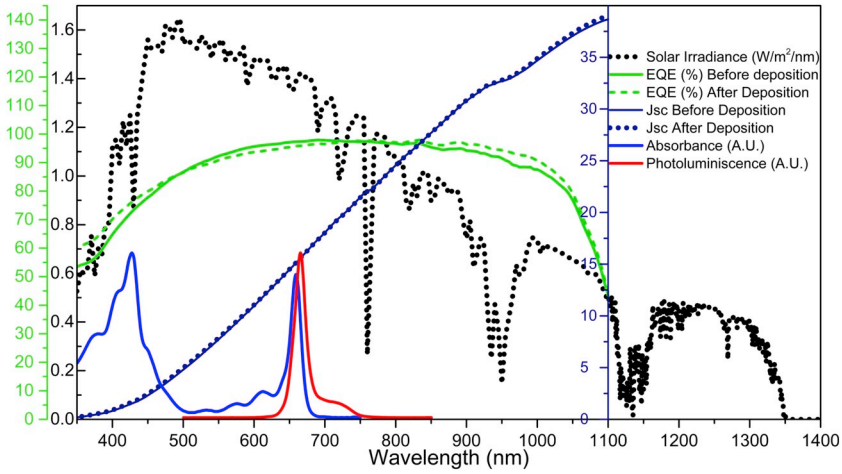

Fig. 13. Measured external quantum efficiency (EQE) of the solar cell before and after (green solid and dashed lines respectively) the deposition of the Chl-A/PMMA 10 μM film and the calculated current density employing the EQE data and Eq. (3) before and after deposition (dark blue solid and dashed lines respectively). Solar irradiance (black dots), chlorophyll-A absorbance (blue) and photoluminescence (red) are also shown as reference. (For interpretation of the references to colour in this figure legend, the reader is referred to the web version of this article.)

To further investigate the influence of chlorophyll-A in the performance of the photovoltaic devices, the external quantum efficiency (EQE) was also measured. This study provides the spectral response of the solar cells with and without the luminescent layer in the wavelength range from 300 nm to 1100 nm (see Fig. 13). The photovoltaic response was improved in the high photon energy region, i.e., below 500 nm, as well as in the relatively low photon energy region with wavelengths above 850 nm. The improvement in the high photon energy region is thought to be produced by the photoluminescent effect of chlorophyll-A, while the improvement in the low photon energy region could be attributed to a change in the reflectance attributable to the presence of the Chl-A/PMMA film. Additionally, the EQE results can provide a corroboration of the photovoltaic performance improvement by the calculation of the current density employing the following equation [36]:

$$J_{sc} = q \int b_s(E) EQE(E) dE \quad (3)$$

where q is the electron charge, $b_s(E)$ is the incident spectral photon flux density and $EQE(E)$ is the measured external quantum efficiency. The calculated current density values employing Eq. (3) are also shown in Fig. 13. These results are in agreement with the values measured in the I–V characterization confirming the improvement of the generated photocurrent.

4. Conclusions

Chlorophyll-A/PMMA has been characterized as a promising photoluminescent material and employed as a down-shifting layer on silicon based solar cells. A relative straightforward method has been employed for the extraction and redispersion of chlorophyll in a PMMA matrix host. The statistically significant collected data suggests that the incorporation of the chlorophyll-A/PMMA layer on the window side of photovoltaic devices produces an improvement of the photocurrent generation and hence, an increment in the power conversion efficiency of the solar cells. An improvement of up to 2.23% of the overall PCE was observed in solar cells after the deposition of Chl-A/PMMA films with a10μM concentration, triggering increases in the PCE from 15.27% to 15.61%. The methods described herein, represent a promising strategy towards the improvement of silicon based solar cells efficiencies, which could be reflected as an impulse on the solar energy harvesting.

Acknowledgements

The authors would like to acknowledge the U.S. Army Research Office [Grant W911NF-13-1-0110], NSF [Grant 1650571], CONACYT [Cátedra No. 529], the Department of Physics and Astronomy at the University of Texas at San Antonio and the Physics Department of the University of Sonora, for the financial support provided for this research project.

References

[1] N.S. Lewis, D.G. Nocera, Powering the planet: chemical challenges in solar energy utilization, Proc. Natl. Acad. Sci. 103 (43) (2006) 15729–15735.
[2] O. Morton, Solar energy, A new day dawning?: Silicon Valley sunrise, Nature 443 (7107) (2006) 19–22.
[3] L.C. Hirst, N.J. Ekins-Daukes, Fundamental losses in solar cells, Prog. Photovolt. Res. Appl. 19 (3) (2011) 286–293.
[4] G.D. Scholes, et al., Lessons from nature about solar light harvesting, Nat. Chem. 3 (10) (2011) 763–774.
[5] X. Huang, et al., Enhancing solar cell efficiency: the search for luminescent materials as spectral converters, Chem. Soc. Rev. 42 (1) (2013) 173–201.
[6] B. Richards, Enhancing the performance of silicon solar cells via the application of passive luminescence conversion layers, Sol. Energy Mater. Sol. Cells 90 (15) (2006) 2329–2337.
[7] B. Qu, et al., Improved performance of a-Si: H solar cell by using up-conversion phosphors, J. Alloys Compd. 658 (2016) 848–853.
[8] B.M. Van Der Ende, L. Aarts, A. Meijerink, Lanthanide ions as spectral converters for solar cells, Phys. Chem. Chem. Phys. 11 (47) (2009) 11081–11095.
[9] T. Trupke, M. Green, P. Würfel, Improving solar cell efficiencies by down-conversion of high-energy photons, J. Appl. Phys. 92 (3) (2002) 1668–1674.
[10] Q. Zhang, X. Huang, Recent progress in quantum cutting phosphors, Prog. Mater. Sci. 55 (5) (2010) 353–427.
[11] M. Stupca, et al., Enhancement of polycrystalline silicon solar cells using ultrathin films of silicon nanoparticle, Appl. Phys. Lett. 91 (6) (2007) 063107.
[12] I. Robel, et al., Quantum dot solar cells. Harvesting light energy with CdSe nanocrystals molecularly linked to mesoscopic TiO2 films, J. Am. Chem. Soc. 128 (7) (2006) 2385–2393.
[13] H.J. Lee, et al., Regenerative PbS and CdS quantum dot sensitized solar cells with a cobalt complex as hole mediator, Langmuir 25 (13) (2009) 7602–7608.
[14] S.-W. Baek, et al., Effect of core quantum-dot size on power-conversion-efficiency for silicon solar-cells implementing energy-down-shift using CdSe/ZnS core/shell quantum dots, Nanoscale 6 (21) (2014) 12524–12531.
[15] R. Lopez-Delgado, et al., Enhanced conversion efficiency in Si solar cells employing photoluminescent down-shifting CdSe/CdS core/shell quantum dots, Sci. Rep. 7 (1) (2017) 14104.
[16] W.B. Hung, et al., Enhanced conversion efficiency of crystalline Si solar cells via luminescent downshifting using Ba2SiO4: Eu2+ phosphor, J. Ceram. Process. Res. 15 (3) (2014) 157–161.
[17] R. Lopez-Delgado, et al., Solar cell efficiency improvement employing down-shifting silicon quantum dots, Microsyst. Technol. 24 (1) (2018) 495–502.
[18] S. Albrecht, et al., Monolithic perovskite/silicon-heterojunction tandem solar cells processed at low temperature, Energy Environ. Sci. 9 (1) (2016) 81–88.
[19] K. Vynck, et al., Photon management in two-dimensional disordered media, Nat. Mater. 11 (12) (2012) 1017.
[20] S. Wiesendanger, et al., A path to implement optimized randomly textured surfaces for solar cells, Appl. Phys. Lett. 103 (13) (2013) 131115.
[21] A. Nozik, Quantum dot solar cells, Physica E: Low-dim. Sys. Nanostruct. 14 (1–2) (2002) 115–120.
[22] D. Timmerman, et al., Space-separated quantum cutting with silicon nanocrystals for photovoltaic applications, Nat. Photonics 2 (2) (2008) 105–109.
[23] B. Moss, Studies on the degradation of chlorophyll a and carotenoids in freshwaters, New Phytol. 67 (1) (1968) 49–59.
[24] V. Rosenbach-Belkin, et al., Chlorophyll and bacteriochlorophyll derivatives as photodynamic agents, Photodynamic Tumor Therapy. 2nd and 3rd Generation Photosensitizers, 1998, pp. 117–125.

[25] J.A. Elemans, et al., Molecular materials by self-assembly of porphyrins, phthalocyanines, and perylenes, Adv. Mater. 18 (10) (2006) 1251–1266.
[26] Y. Saga, et al., Structure-dependent Demetalation kinetics of chlorophyll a analogs under acidic conditions, Photochem. Photobiol. 89 (1) (2013) 68–73.
[27] Y.-R. Kang, et al., Synthesis, characterization, and functional properties of chlorophylls, pheophytins, and Zn-pheophytins, Food Chem. 245 (2018) 943–950.
[28] E.M. Reol, Los pigmentos fotosintéticos, algo más que la captación de luz para la fotosíntesis, Rev. Ecosistemas 12 (1) (2003).
[29] D. Yu, et al., Enhanced photocurrent production by bio-dyes of photosynthetic macromolecules on designed TiO 2 film, Scientific Reports, vol. 5, 2015, p. 9375.
[30] A. Mershin, et al., Self-assembled photosystem-I biophotovoltaics on nanostructured TiO 2 and ZnO, Scientific Reports, vol. 2, 2012, p. srep00234.
[31] L.O. Björn, G.C. Papageorgiou, R.E. Blankenship, A viewpoint: why chlorophyll A? Photosynth. Res. 99 (2) (2009) 85–98.
[32] J.J. Lamb, J.J. Eaton-Rye, M.F. Hohmann-Marriott, An LED-based fluorometer for chlorophyll quantification in the laboratory and in the field, Photosynth. Res. 114 (1) (2012) 59–68.
[33] M. Taniguchi, H. Du, J.S. Lindsey, PhotochemCAD 3: diverse modules for photophysical calculations with multiple spectral databases, Photochem. Photobiol. 94 (2) (2018) 277–289.
[34] J.M. Dixon, M. Taniguchi, J.S. Lindsey, PhotochemCAD 2: a refined program with accompanying spectral databases for photochemical calculations, Photochem. Photobiol. 81 (1) (2005) 212–213.
[35] G. Beadie, et al., Refractive index measurements of poly (methyl methacrylate) (PMMA) from 0.4–1.6 μm, Appl. Opt. 54 (31) (2015) F139–F143.
[36] J. Nelson, The Physics of Solar Cells, World Scientific Publishing Company, 2003.